Absolute Radiometric Calibration of Planet Dove Satellites, Flocks 2p & 2e

Nicholas Wilson[1], Joshua Greenberg[1], Arin Jumpasut[1], Alan Collison[1], Horst Weichelt[2]

[1]Planet Labs, 346 9th St, San Francisco, CA 94103

[2]Planet Berlin GmbH, Kurfürstendamm 22, 10719 Berlin, Germany

nick.wilson@planet.com

joshua.greenberg@planet.com

arin.jumpasut@planet.com

alan.collison@planet.com

horst.weichelt@planet.com

Table of Contents

Introduction

This document summarizes the methods and results of the radiometric calibration update applied to 38 Dove satellites on the 30th of March, 2017. The satellites were part of Flock 2p, a group of 12 satellites in Sun-synchronous (SSO) orbit and Flock 2e, a group of 26 satellites in International Space Station (ISS) orbit. Flock 2p was deployed in June, 2016 and Flock 2e was deployed in 3 separate groups from the International Space Station between May and September, 2016. This was the first update to the radiometric calibration of Planet Dove satellites using on-orbit methods and the update is retroactive to the analytic product catalog of these satellites. The update corrects for systematic bias in the per-band calibration and minimizes relative differences between Dove satellites. The radiometric uncertainty across all satellites in these groups is measured at 5-6% at 1-sigma after this calibration update.

Calibration Approach

A hybrid methodology was developed for on-orbit radiometric calibration of the Planet Dove satellites that combines lunar calibration with instantaneous crossovers with RapidEye and Landsat 8 in pseudo-invariant calibration sites (PICS). The approach utilized data in radiance units (W/(m² sr μm)) and normalized for reference sensor differences and time of day effects to produce absolute radiometric corrections for each sensor. Lunar and Cross-calibration data were compiled over a period of 6 months and reference data covered the dynamic range of each sensor from 5 to 150 W/(m² sr μm). Uncertainty in the model fitting was minimized by the quantity of data used to derive calibration models, and on average 800 radiometric sample points were used to fit the calibration models for each sensor.

A primary requirement of the method was that most of the data processing could be automated given the number of satellites in the constellation and the need for regular temporal radiometric monitoring into the future. The automated approach included tasking RapidEye for predicted crossovers with Planet Dove Satellites in calibration sites, scheduling moon shots during each monthly moon phase, and processing imagery from all methods in the imaging pipeline. The process captures and stores calibration data in a standardized format, allowing for monthly monitoring of the radiometric calibration of each satellite and the ability to update the calibration on a semi-regular basis.

Lunar Calibration

Lunar calibration is a well documented approach for on-orbit radiometric calibration and has been used by a wide range of Earth Observation instruments [1]. The moon is considered an ideal calibration target due to its lack of atmosphere, radiometric stability, and regularity in which it can be imaged for calibration purposes. This approach uses radiometric reference data derived from the USGS RObotic Lunar Observatory (ROLO) model. An implementation of this model was developed based on Stone et al. 2005 [2].

Moonshots

In order to acquire adequate lunar data for calibration, each satellite carried out daily moon shots during a full lunar cycle, both waxing and waning phases. Figure 1 illustrates the daily moon shots taken by a single satellite across a month-long moon phase.

Figure 1: Compilation of a full moon phase taken by a Dove Satellite.

An example of how measured radiances (extracted from imagery) scale by moon phase angle (defined as the angle between the satellite, the moon, and the sun) is provided if Figure 2. As the moon phase progresses from ‘New Moon’ to ‘Full Moon’ and then back to ‘New Moon’, the overall radiance increases and then decreases across the lunar cycle. Using the ROLO model as radiance reference by phase angle allows for reliable calibration data to be collected by each satellite every month.

The general processing steps for moon shots is as follows:

1. Image taken of the moon when the satellite is in eclipse.
2. Image downlinked and tagged as a moon shot in the imaging pipeline.
3. Ellipse finding algorithm identifies the moon in the image and extracts the moon pixels.

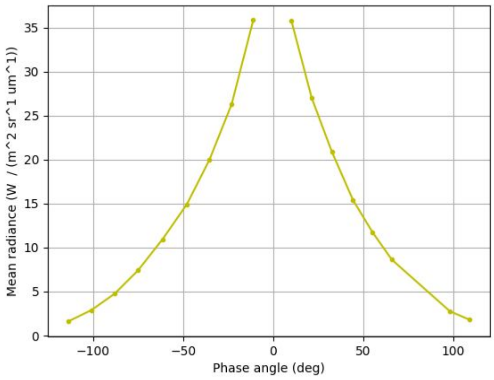

Figure 2: Radiance (W/(m² sr μm)) by moon phase angle across a lunar cycle.

4. Moon pixel values in radiance W/(m² sr μm) are summed and summary statistics stored.
5. ROLO moon-disk integrated radiance and mean radiance is calculated based on the phase angle of the moon at the time of image acquisition and pixel count.
6. Invalid scenes within the moon collect are flagged based on the radiance measurement compared to the overall trend of the collect.
7. All source and reference radiance values are stored in the database.

Cross-calibration

Cross-calibration is an approach that utilizes near instantaneous crossovers with well calibrated satellites to define the radiometric reference dataset. RapidEye and Landsat 8 were selected as reference sensors for this process. RapidEye maintains annual vicarious campaigns and quotes a radiometric accuracy of 4% [3]. Landsat 8 has on-board calibration lamps as well as annual vicarious campaigns with a quoted radiometric accuracy at 4% [4].

Dove to Dove crossovers were also utilized for select satellites that did not have adequate crossovers with RapidEye and Landsat 8. In these cases, Dove satellites with adequate crossovers were chained together with satellites that did not have enough data so that sufficient crossover data was available for calibration model fitting.

Calibration Sites

The calibration sites used for the evaluation were distributed globally in both the northern and the southern hemispheres. The 25 sites are a combination of locations that RapidEye team uses for temporal radiometric calibration, which are known to be stable and homogeneous, as well as the internationally used invariant calibration sites known as “PICS”. All sites have very low vegetation cover and therefore show a minimum dependency on the vegetation cycle.

The calibration sites can generally be described as desert environments comprised of bright soil. For each Planet Dove satellite, crossover samples were acquired across the widest range of brightnesses in order to provide sufficient variation in the ground object brightness and illumination conditions. Table 1 provides more detail on each site, including locations and site descriptions.

Table 1: Calibration site descriptions.

Name	Lat / Lon	Description
Algodones Dunes	33/ -115	Desert (Sonoran), dunes at multiple scales and homogenous with little vegetation
Australia C	-25/ 138	Flat, dry, somewhat homogeneous, almost no vegetation.
Arizona	37/ -109	Desert (Sonoran), flat, dry, small, fairly homogeneous, no vegetation.
Bolivia	-20 / -67	Salt Desert, flat, dry, fairly homogeneous and very bright, no vegetation.
China-A	43 / 109	Desert (Gobi), partly steppe, dry ,large, less vegetation, mountainous
China-B	41 / 104	Desert (Gobi), dry, large, some sand dunes, mountainous, no vegetation
Dunhuang	40 / 94	Desert (Gobi), flat, dry, overall homogeneous, no vegetation. Possibly affected by atmospheric aerosol due to sandstorms and dust.
Egypt A	16 / 27	Desert, flat, dry, large, homogeneous, no vegetation.
Egypt B	25 / 29	Desert, flat, dry, large, homogeneous, no vegetation.
Egypt 1	27/ 26	Desert, flat, dry, large, patchy across larger areas.
Libya	27 / 13	Desert (Sahara), flat, dry, large, dunes at multiple scales, but overall homogeneous, no vegetation.

Libya4	29 / 23	Desert (Sahara), flat, dry, large, dunes at multiple scales, but overall homogeneous, no vegetation.
Libya1	25 / 13	Desert (Sahara), flat, dry, large, dunes at multiple scales, but overall homogeneous, no vegetation.
Niger 1	20 / 10	Desert (Sahara), flat, dry, large, dunes at multiple scales, but overall homogeneous, no vegetation.
Niger 2	21 / 11	Desert (Sahara), flat, dry, large, dunes at multiple scales, but overall homogeneous, no vegetation.
Mauritania	21 / -12	Desert (Sahara), flat, dry, large, dunes at detailed scales, but overall reasonably homogeneous areas, large dunes at northern part.
Mexico	33/ -115	Desert (Sonoran), flat, dry, dunes, homogenous, NW corner agricultural areas
Namibia	-16 / 12	Desert, flat, dry, large, somewhat homogeneous, no vegetation.
SaudiArabia	29 / 45	Desert, flat, dry, dune patterns at several scales, but homogeneous when averaged over larger areas, no vegetation.
Sudan-A	27 / 29	Desert, flat, dry, large, patchy across larger areas.
Sudan-B	23 / 28	Desert (Sahara), flat, dry, large, somewhat patchy but overall reasonably homogeneous areas of smaller size.
Sudan-C	15 / 27	Desert, flat, dry, large, homogeneous, no vegetation.
Sudan 1	22 / 28	Desert, flat, dry, large, homogeneous, no vegetation.
Railroad Valley	38/ -115	Dry-lake playa, flat, small, but spatially uniform.
Taklamakan	40 / 80	Desert, flat, dry, large, dunes at multiples scales, but overall homogenous

Calibration Site Spectra

As the calibration update utilized a radiance approach, normalizing for the different relative response of each sensor was required. Each sensor has a unique relative spectral response and even well calibrated sensors will produce different radiance values because they are sensitive to different parts of the spectrum. Having detailed spectra of calibration sites enables the conversion of an image taken by one sensor into an image that the corresponding reference sensor would record. This correction utilizes a per-band spectral band adjustment factor (SBAF) [5]. A comparison of the relative spectral response between a Planet Dove Satellite, RapidEye, and Landsat 8 are shown in Figures 3 and 4 respectively.

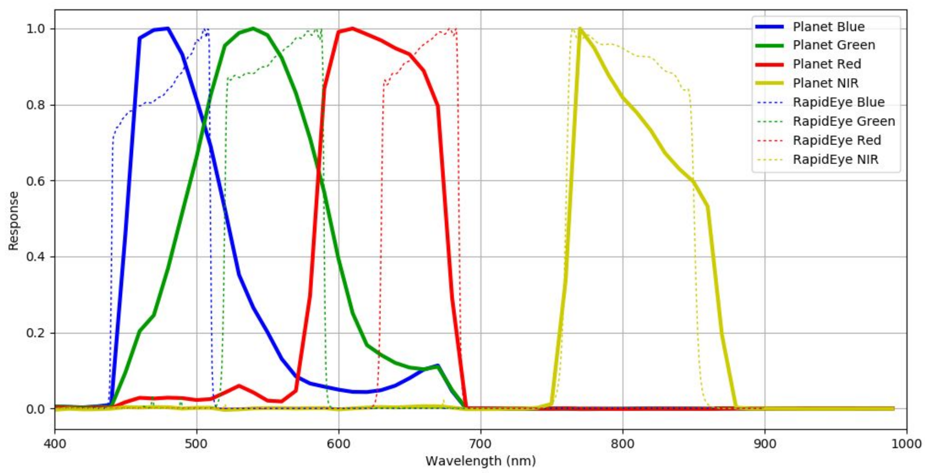

Figure 3: Planet Dove and Rapideye RSR comparison.

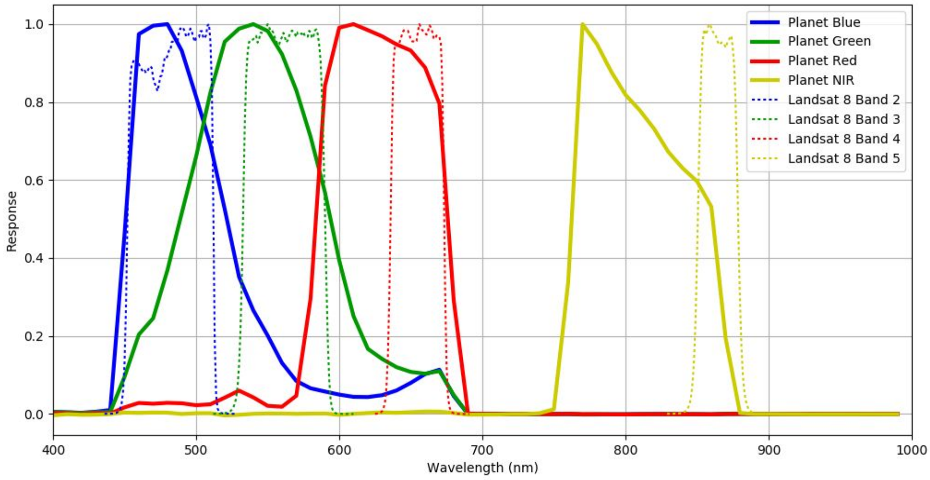

Figure 4: Planet Dove and Landsat 8 RSR comparison. Note the large difference in NIR bands.

In order to minimize error in the calculation of the SBAF, each calibration site was characterized using Hyperion hyperspectral data and an average spectra derived for each site. Site spectra were created by averaging 12 overlapping Hyperion scenes, 1 from each month of the year in order to capture seasonality effects. This average image was then sampled across the areas of the site used for crossover sampling, aggregated to per-band sample averages, and normalized into 10 nm radiance spectra.

Instantaneous Crossovers and Corrections

An instantaneous crossover is when 2 satellites image the same place on the Earth at effectively the same time. The crossover quality criteria used for both RapidEye and Landsat 8 crossovers with Dove satellites included:

- Crossover must occur within a characterized calibration site.
- Maximum time delta of 2 hours between crossover images.
- Maximum 10 degree view angle of the reference satellite (Doves are always nadir pointing).
- Maximum of 20% of pixels saturated in any one band for any image.
- Maximum of 20% clouds in for any image.
- Any pixels with NDVI > 0.2 (vegetation) in either image are masked.
- All saturated and cloud pixels must be masked.

Using the above criteria to define the location and required attributes of crossover image pairs, a number of processing steps and corrections were applied to extract comparable samples for use in calibration. These steps included:

1. Process image pairs to Top of Atmosphere Radiance, normalized to 4-meter spatial resolution.
2. Intersect crossover image pairs, extracting only the locations of shared information.
3. Extract sample images of each sample pair using predefined 1000 x 1000 pixel sampling grid. Figure 5 provides an example of crossover sampling in the Algodones Dunes calibration site.

4. For each reference image sample, apply spectral band adjustment factor (SBAF) correction. For each band, the SBAF was calculated with the following equation:

$$SBAF_{1\rightarrow 2,b} \equiv \frac{\left(\frac{\int \varrho(\lambda)\, RSR_{2,b}(\lambda)\, d\lambda}{\int RSR_{2,b}(\lambda)\, d\lambda}\right)}{\left(\frac{\int \varrho(\lambda)\, RSR_{1,b}(\lambda)\, d\lambda}{\int RSR_{1,b}(\lambda)\, d\lambda}\right)}$$

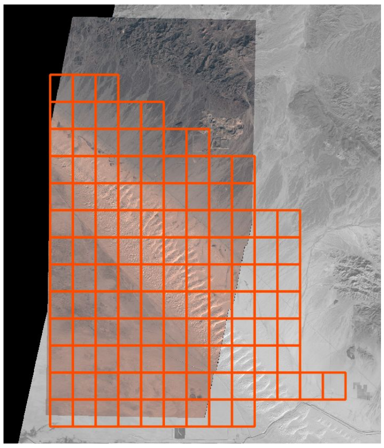

Figure 5: Example of crossover event with sampling grid overlaid in Algodones Dunes calibration site.

5. Apply sun angle correction to adjust for time of day differences between crossover image pairs. The sun angle correction used the following equation:

$$R_{LSatLcor} = R_{LsatLorig} * \frac{\cos(1-\theta_{SunPL})}{\cos(1-\theta_{SunLsat})} ,$$

where:

R = radiance,

θ_{Sun} = sun elevation angle

6. Calculate summary statistics for each band within the sample images and record in the database.

Calibration Update

In order to produce updated calibration gains and offsets, absolute calibration adjustment factors were derived for each sensor. The factors were derived by combining lunar and cross calibration datasets into a single population of samples by sensor. It was found that both radiometric reference sources were linear and in the same direction, whether the data was sourced from the ROLO model or from RapidEye/Landsat 8 crossovers. The benefit of combining datasets was that the sample data filled the entire operational dynamic range of each sensor, from 5 to 150 W/(m² sr µm). Lunar-derived calibration data populated the lower end of the dynamic range, from 5 to 50 W/(m² sr µm), and cross calibration data filled the top end of the dynamic range, from 50 to 150 W/(m² sr µm).

To finalize the model fit for each sensor, the combined sample data was filtered for outliers. Outliers included points that had residual clouds, significant shadow differences between crossover times, BRDF effects, low SNR, and overly heterogeneous ground cover. Criteria used for filtering outliers included:

- No samples > 15% different between source and reference.
- Standard deviation of radiance values within sample for either source or reference < 3 W/(m² sr µm).

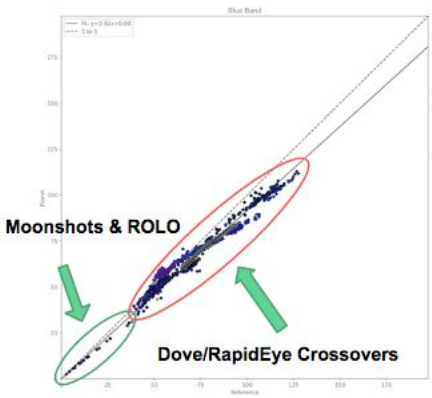

Figure 6: Example calibration model combining Lunar and Cross Calibration datasets.

Having filtered for outliers, calibration models were fitted using the RANSAC algorithm which provides an additional level of resistance to outliers. Using the fit, adjustment factors were derived to force the fit line to unity and then applied to generate updated calibration coefficients.

Evaluating Radiometric Accuracy

Evaluation of the updated calibration model for each satellite included the calculation of absolute accuracy, standard error of the accuracy, and the uncertainty (standard deviation of the percent errors), as well as a visual assessment of the plot data for any bias across the radiance range. Table 2 provides an overview of the accuracy assessment across all updated satellites, including mean absolute accuracy and uncertainty values.

Table 2: Average constellation radiometric accuracy after on-orbit update.

FLOCK 2e & 2p					
	Avg. magnitude of change from Gen 1	Mean Absolute Accuracy	Average Uncertainty (Stdev of Percent Errors)	Minimum Uncertainty (Of any satellite)	Maximum Uncertainty (Of any satellite)
blue	7.14%	0.14	4.30	2.54	5.55
green	7.80%	0.17	4.07	2.72	6.14
red	6.55%	-0.47	4.12	2.42	6.27
nir	5.93%	-0.55	4.74	2.84	6.49

Due to the choice of using the RANSAC algorithm for model fitting, which uses a subset of the data (inliers) to derive the calibration model, the mean absolute accuracy slightly deviates from 0 after the calibration update because all sample points are included in the calculation. The uncertainty provides an assessment of how spread out the data was in terms of percent error at 1-sigma. The maximum uncertainty for any band, for any satellite is 6.49 (in the NIR band). Given the overall average uncertainty is between 4-5% for any band, and accounting for the subset of satellites which have uncertainties closer to the maximum, it is reasonable to conclude that the uncertainty of the calibration is 5-6% at 1-sigma for the constellation.

The relative impact of the radiometric calibration update is provided in the figures below. Figure 6 shows the pre-corrected accuracy and uncertainty by satellite while Figure 7 displays the corrected radiometric accuracy and uncertainty by satellite. The visible difference in the two plots, before and after on-orbit calibration correction, shows the radiometric calibration for each satellite improves relative to reference on average, and in some cases also improves in terms of the spread of values.

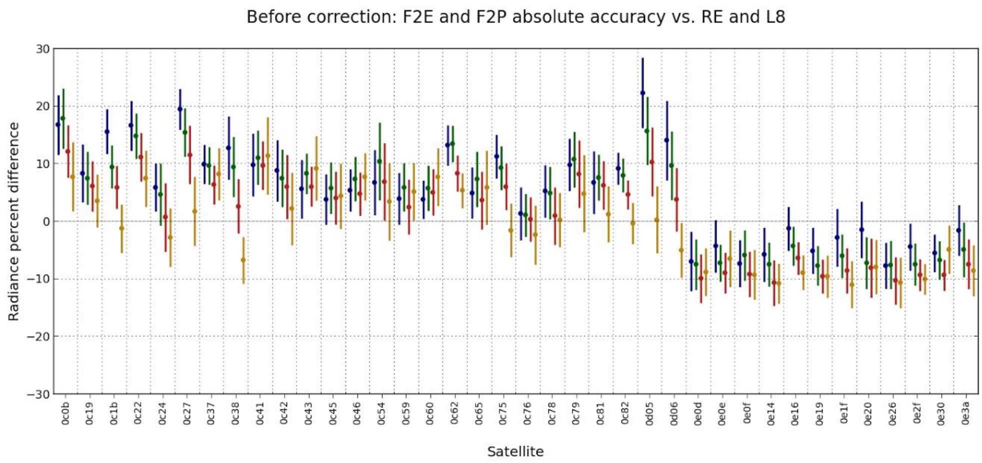

Figure 7: Pre-calibration update accuracy and uncertainty at 1-sigma (standard deviation of percent errors) per-band, by satellite. Flock 2e satellites have 0c* names while F2p have 0e* names.

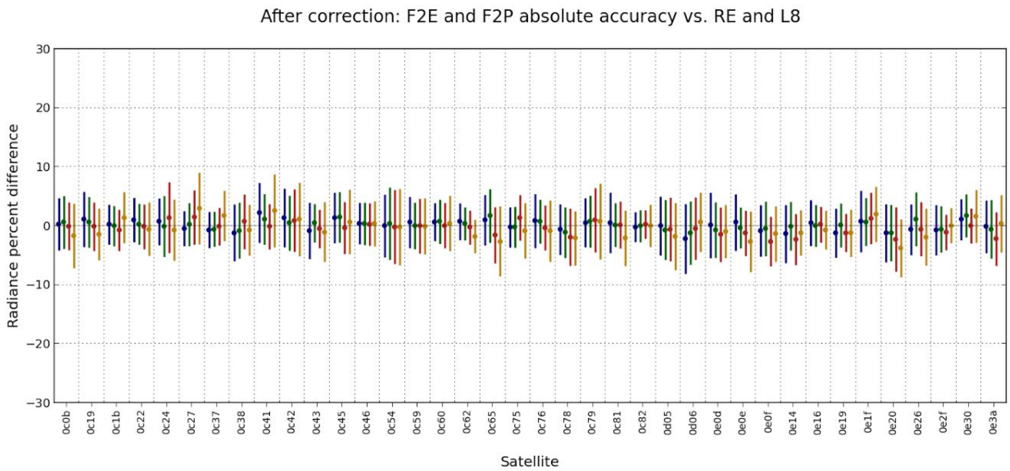

Figure 8: On-orbit calibration update accuracy and uncertainty at 1-sigma (standard deviation of percent errors) per-band, by satellite. Note that all satellites are now on the same calibration scale after the update.

The center of the bar is the mean percent error with respect to reference, and the bar extends upwards to Accuracy + Uncertainty and downwards to Accuracy - Uncertainty, representing a spread of +-1 standard deviation of percent errors. Since the reference radiances are assumed, on average, to give us the top of atmosphere radiance truth (respectively the mean lunar radiance truth), the rough interpretation of each bar is "How close is the Planet Dove radiometric calibration to truth", both on average (the center of the bar), and in terms of the spread of values (the size of the bar top to bottom). The band groupings allow for an assessment of each satellite calibration as well as insight into the relative differences across the constellation. In both cases, the on-orbit update significantly aligns the radiometric calibration to absolute truth and minimizes relative differences between satellites and aligns them to the same uncertainty range.

Absolute Radiometric Validation

Using a validation dataset derived from the RADCALNET Railroad Valley automated calibration site, a vicarious approach was utilized to validate the calibration for a subset of satellites. RADCALNET provides SI-traceable Top-of-Atmosphere (TOA) spectrally-resolved reflectances and intends to capture spectral data at 30 minute intervals during daylight hours each day. There were 26 collects of the Railroad valley site by the satellites included in this update, but only 12 collects had corresponding RADCALNET data taken within 15 minutes of the Dove images. These 12 collects were captured by 7 different satellites and represent only a sample of the satellites included in the on-orbit update.

The images were processed to TOA reflectance for comparison to the RADCALNET reference. The RADCALNET data provided TOA reflectance at 10 nm spectral resolution and was processed to extract the equivalent Dove TOA reflectance by convolving the sensor RSR with the spectrally resolved reflectances. A comparison of the pre-launch calibration and on-orbit calibration in terms of absolute accuracy and uncertainty is provided in Table 3.

Table 3: Comparison of accuracy statistics before and after on-orbit update.

	Pre-launch Calibration (Gen 1)			**On-Orbit Calibration - Post Update (Gen 2)**	
Band	Absolute Accuracy	Uncertainty (1-sigma)		Absolute Accuracy	Uncertainty (1-sigma)
Blue	-8.26	3.84		-5.15	4.33
Green	-7.59	4.18		-1.08	4.61
Red	-7.71	3.58		0.0005	3.48
NIR	-10.36	4.89		-3.50	3.76

Overall, the radiometric accuracy improves in absolute terms after the on-orbit update, without any significant change in the uncertainty. The relative radiometric accuracy (between satellites) also improves based on these results and are in line with the findings of the relative calibration results derived from the calibration model fits. With only 13 samples of the Railroad Valley site, and no more than 2 samples from any single satellite, the collects have a low sample size and represent only a narrow window of the dynamic range. This should be taken into account when interpreting these results.

The absolute accuracy of blue band is higher than expected but this can likely be explained by atmospheric effects, by atmospheric modelling uncertainty in the RADCALNET data, and by seasonality effects. Most of the collects occurred in winter months during periods of significant water being mixed in the soil. Further analysis of this difference will be analyzed as more data is available. The distribution of percent errors by TOA reflectance range is provided in Figure 9.

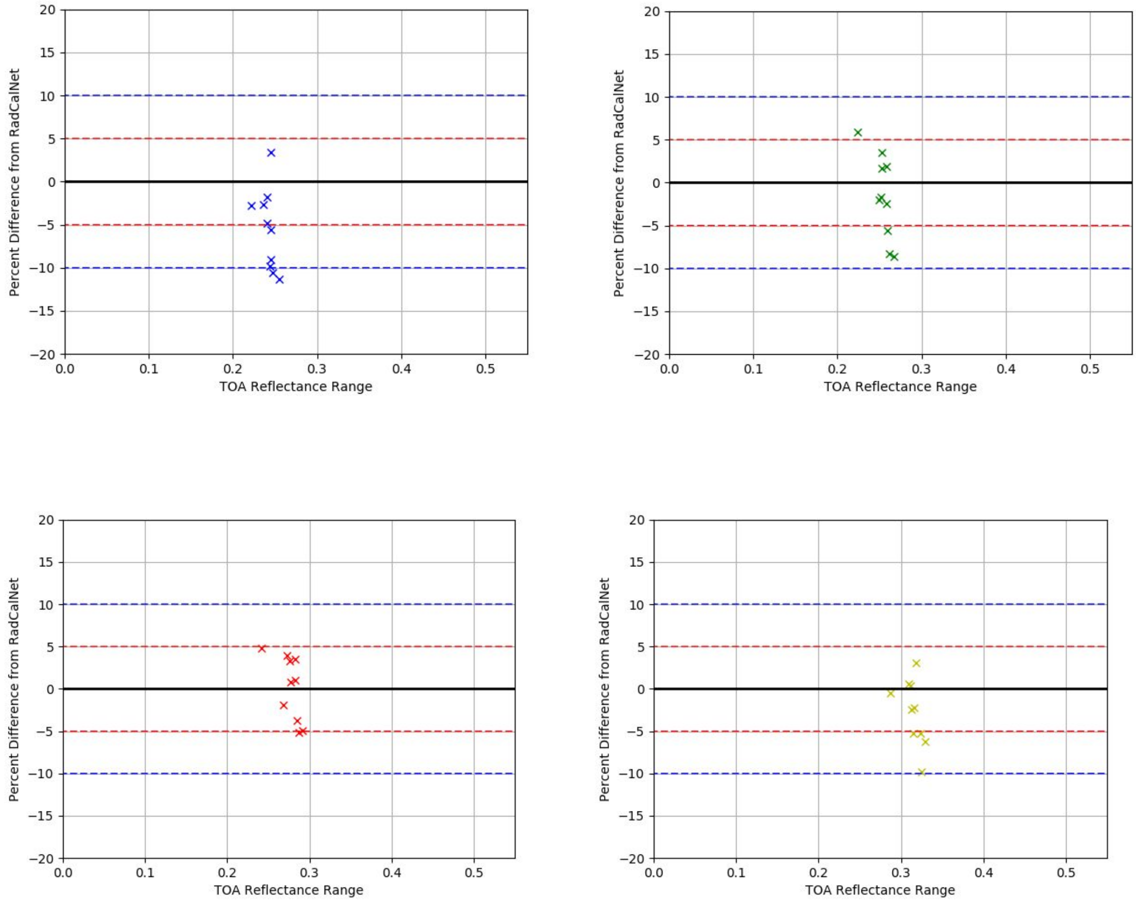

Figure 9: Distribution of TOA reflectance by percent error. Note the Railroad Valley site is in the bottom third of the reflectance range.

The distribution of samples for each band show the limited dynamic range that is covered by only using the Railroad Valley calibration site. Apart from the blue band, all other bands show a reasonable distribution +-5% from RADCALNET reference, with the entire distribution of points within 10%.

Conclusion

This process has enabled an automated approach that has improved the radiometric calibration of the Planet Dove satellites from a constellation uncertainty of 20% to a 5-6% uncertainty at 1-sigma. Further validation using a small sample of vicarious data from the Railroad Valley RADCALNET site supported this finding, with all bands having an absolute accuracy within the quoted uncertainty after the calibration update. Further monitoring of the radiometric calibration will be ongoing, with regular monthly moon shots for each satellite and daily processing of tasked and opportunistic crossovers with RapidEye and Landsat 8. Long term, additional crossovers will be processed with Sentinel 2. There will also be continued work on vicarious calibration approaches to support further refinements in the scaled radiometric calibration of large constellations of Planet Dove satellites.

References

[1] T. C. Stone, “Radiometric calibration stability and inter-calibration of solar-band instruments in orbit using the moon,” in Optical Engineering+ Applications, 2008, p. 70810X–1–8.

[2] H. H. Kieffer and T. C. Stone, “The spectral irradiance of the Moon,” The Astronomical Journal, vol. 129, no. 6, pp. 2887–2901, 2005.

[3] D. Naughton et al., “Absolute radiometric calibration of the RapidEye multispectral imager using the reflectance-based vicarious calibration method,” Journal of Applied Remote Sensing, vol. 5, no. 1, pp. 53544–53544, 2011.

[4] B. Markham et al., “Landsat-8 Operational Land Imager Radiometric Calibration and Stability,” Remote Sensing, vol. 6, no. 12, pp. 12275–12308, Dec. 2014.

[5] G. Chander et al., “Applications of spectral band adjustment factors (SBAF) for cross-calibration,” Geoscience and Remote Sensing, IEEE Transactions on, vol. 51, no. 3, pp. 1267–1281, 2013.